

Influence of Strain Rate on the Effect of Plasticization of High-Strength Ultrafine-Grained Al–Cu–Zr Alloy

© D.I. Sadykov¹, T.S. Orlova^{2,¶}, M.Yu. Murashkin³

¹ ITMO University,
St. Petersburg, Russia

² Ioffe Institute,
St. Petersburg, Russia

³ Institute of Physics of Advanced Materials, Ufa State Aviation Technical University,
Ufa, Russia

¶ E-mail: orlova.t@mail.ioffe.ru

Received February 22, 2022

Revised February 22, 2022

Accepted February 24, 2022

The influence of the strain rate on the plasticization effect (PE) of ultrafine-grained (UFG) Al–1.47Cu–0.34Zr (wt%) alloy structured by high pressure torsion. A significant increase in plasticity (more than 2 times) while maintaining a high level of strength (ultimate tensile strength ~ 465 MPa) in the UFG alloy was achieved as a result of additional deformation-heat treatment (DHT), consisting of low-temperature annealing and a small additional deformation. It is shown that the PE after DHT is retained when the strain rate changes from 10^{-4} to 10^{-3} s⁻¹ and decreases by half with its further increase to 10^{-2} s⁻¹. The values of the strain-rate sensitivity coefficient for the UFG Al–1.47Cu–0.34Zr (wt%) alloy were determined in both states before and after DHT. Possible reasons of the PE suppression at high strain rates ($\geq 10^{-2}$ s⁻¹) are discussed.

Keywords: aluminum alloys, severe plastic deformation, ultrafine-grained structure, strength, plasticity, strain-rate sensitivity.

DOI: 10.21883/PSS.2022.06.54370.297

1. Introduction

Aluminum-based ultrafine-grained alloys (UFG) are of high interest due to their high applicability in aerospace, energy, building and other industries [1]. One of the most effective methods of forming microstructures of this kind is the processing of materials by methods of the severe plastic deformation (SPD) [2]. The materials with a UFG-structure formed by the SPD methods usually exhibit a high level of strength and, in some cases, „superstrength“ [1,3]. A key disadvantage of the UFG-materials is that in most cases they have low plasticity [4], thereby reducing an attractability of their practical use. In connection therewith, presently, a lot of attention is paid to develop scientifically-based approaches aimed at improving the plasticity of high-strength UFG-materials. The examples of these approaches include formation of a bimodal structure [5–8], introduction of nanosized precipitates of the secondary phase [9,10] and etc. [3]. These approaches can be briefly characterized as a microstructure design, i.e. creation of special structures, which provide an increased plasticity in UFG-materials with simultaneously maintaining a high level of the strength.

Fairly recently, we have proposed a new approach to increase the plasticity in the UFG-materials exemplified by the commercially pure aluminum (CP Al). This approach consists in special deformation-heat treatment (DHT), including low-temperature annealing and subsequent additional deformation [11]. The DHT in UFG CP

Al resulted in the increased plasticity in more than two times while maintaining a high level of strength. It is not typical for coarse-grained structures to have the increased plasticity as a result of deformation. It has been shown that the obtained effect of the increased plasticity in UFG CP Al (the plasticization effect (PE)), is associated with introduction of an additional dislocation density to the annealing-relaxed structure of high-angle grain boundaries (GBs). Subsequently, a theoretical model [12,13] had been developed to implement the deformation in UFG Al by emission of the lattice dislocations from the GB, their sliding along the grain and incorporation into the opposite GBs, and to explain the increased plasticity after DHT by introducing the additional density of the grain boundary dislocations (GBDs) into the annealing-relaxed GB structure (by increasing the GB non-equilibrium degree), thereby leading to easier dislocation emission from GBs. The later studies have established PE manifestation in the Al–1.5Cu (wt%) UFG alloy [14]. It aroused not only scientific, but practical interest, as this alloy contains Cu, which is a main alloying element in industrial alloys of the 2xxx series [15,16]. They are widely used as structural materials in various industries [17]. Recently, we have discovered for the first time a similar plasticization effect in the three-component Al–1.47Cu–0.34Zr (wt%) alloy with the UFG-structure [18]. After special DHT including low-temperature annealing and subsequent deformation, the plasticity in this material had increased in more than two

times, which most likely points to versatility of this approach for increasing the plasticity in various aluminum-based UFG alloys.

Nevertheless, in order to implement the proposed approach to increase the plasticity of the Al-based UFG-alloys, it is necessary to deeply study the physical nature of this phenomenon, since at the present stage of the studies the proposed theoretical model is not versatile and has been developed, first of all, for pure Al. This model has not included impact of alloying elements, which, as is known [19–21], can significantly affect mechanisms of the plastic deformation. In order to better understand the physical nature of the plasticity increase effect due to the deformation, it is important to study the impact of external factors thereupon, such as a strain rate and temperature of tensile test. Moreover, such studies are also important in terms of practical use to reveal those temperature and rate conditions, which are suitable for making parts or products from high-strength UFG-alloys using various deformation methods, and to determine possible operating conditions thereof, as well.

It is known that the Al-based UFG-alloys exhibiting not only high plasticity, but even superplasticity in some cases, were highly sensitive to the strain rate [1,19,22–24]. In accordance with the known Hart criterion [25], the uniform deformation transforms to a deformation localization stage provided that:

$$\frac{d\sigma}{d\varepsilon} \leq (1 - m) \cdot \sigma, \quad (1)$$

where σ — the flow stress, ε — the plastic deformation, $m = \frac{d \ln \sigma}{d \ln \dot{\varepsilon}}$ — the strain-rate sensitivity coefficient, $\dot{\varepsilon}$ — the strain rate, $\frac{d\sigma}{d\varepsilon}$ — strain hardening rate (strain hardening coefficient)

It is obvious that at quite big values of m the material can effectively withstand heterogeneous deformation even without significant deformation strengthening. The increased value of the coefficient m is usually correlated to activated grain boundary sliding, which results in more uniform microplastic flow in the sample preventing macro-localization processes with neck formation. It provides for increased plasticity [26,27] or even leads to superplasticity at the room temperature, as it was observed, for example, for the Al–30Zn (wt%) UFG-alloy [19].

The present paper has investigated impact of the tensile strain rate at the room temperature on the plasticization effect in the Al–1.47Cu–0.34Zr (wt%) UFG-alloy, which is structured by the high pressure torsion (HPT) and subjected to special DHT as per a mode, which has been proposed by the authors in the previous study [18].

2. Materials and experimental methods

The present paper investigates the Al–1.47Cu–0.34Zr (wt%) alloy (hereinafter referred to as the Al–Cu–Zr alloy), which is produced by casting and subsequent cold rolling as a cylinder bar of the diameter of 14.5 mm [28]. In

order to form the UFG-structure, the blank cylinders of the height 3 mm and the diameter 14.5 mm, pre-aged by long annealing at 375°C during 140 h, were subjected to high pressure torsion (HPT) using the Walter Klement GmbH HPT-07 press. The samples were structured by the HPT at the room temperature (RT) under the hydrostatic pressure of 6 GPa at a number of revolutions of $n = 10$. It resulted in producing discs of the diameter of ~ 20 mm and the thickness of ~ 1 mm. The true strain (ε) at the distance of 5 mm from the disc center was ~ 6.6 [28,29]. Hereinafter, this state of the samples is designated as AG + HPT.

Some samples in the AG + HPT state were subjected to deformation-heat treatment (DHT) consisting in annealing at the temperature of 125°C during 240 min (hereinafter, this state is designated as AG + HPT + AN), and subsequent additional deformation by the RT HPT at the pressure of 6 GPa and $n = 0.25$, which corresponds to $\varepsilon \sim 0.025$ (hereinafter, this state is designated as AG + HPT + AN + 0.25HPT). We have previously demonstrated that this DHT mode leads to significant increase (in more than two times) in the plasticity of the material under study with UFG-structure in uniaxial tensile tests at the strain rate of $5 \cdot 10^{-4} \text{ s}^{-1}$ at the room temperature [18].

In the present paper, the uniaxial tensile tests were performed at the room temperature at the strain rates of 10^{-4} , $5 \cdot 10^{-4}$, 10^{-3} and 10^{-2} s^{-1} using the Shimadzu AG-50kNX machine. Blade-shaped samples with the gauge sizes of $2.0 \times 1.0 \times 6.0$ mm were used as in the study [30]. Preparation of the samples for the mechanical tests, including a sample cut diagram is detailed in the paper [28]. The sample deformation was measured using the TRViewX 55S video-extensometer. At least three samples were tested for each strain rate. The obtained stress–strain curves allowed determining the ultimate tensile strength (σ_{UTS}), the conventional yield stress ($\sigma_{0.2}$), the elongation to failure (δ), the uniform elongation (δ_1) and the strain-rate sensitivity coefficient (m).

3. Experimental results and discussion

The microstructure studies of samples of the Al–Cu–Zr alloy in the AG + HPT, AG + HPT + AN, AG + HPT + AN + 0.25HPT states have been carried out by us earlier using the transmission electron microscopy and scanning electron microscopy, energy dispersive spectroscopy (EDS) and the X-ray diffraction (XRD) analysis [18,28]. The main microstructure parameters are given in Table 1.

The papers [18,28] have established that HPT-treatment of the Al–Cu–Zr alloy led to formation of the UFG-structure with an average grain size of $d_{av} \approx 285$ nm. There was an insignificant quantity of precipitates of the Al₃Zr secondary phase with the average size of ~ 17 nm, which were predominantly located in the grain interior. Precipitates of the Al₂Cu secondary phase with the sizes of 20–40 nm were observed at the grain boundaries. After low-temperature

Table 1. Microstructure parameters of samples of the Al–1.47Cu–0.34Zr (wt%) UFG-alloy in the different states [18]

| State | d_{av} , nm | D_{XRD} , nm | $\langle \varepsilon^2 \rangle^{1/2}$, % | L_{dis} , 10^{13} m^{-2} | a , Å |
|-------------------------|---------------|----------------|---|--------------------------------------|----------------------|
| AG + HPT | 285 ± 23 | 205 ± 1 | 0.044 ± 0.002 | 2.6 | 4.0504 ± 0.00006 |
| AG + HPT + AN | 360 ± 25 | 295 ± 4 | 0.042 ± 0.0003 | 1.7 | 4.0500 ± 0.00003 |
| AG + HPT + AN + 0.25HPT | 315 ± 24 | 211 ± 4 | 0.052 ± 0.001 | 3.0 | 4.0502 ± 0.00006 |

annealing at 125°C during 240 min (the AG + HPT + AN state), the average grain size was insignificantly increased (~ 360 nm), while the average size of the Al₂Cu precipitates was ~ 60 nm. After additional deformation (the AG + HPT + AN + 0.25HPT state), the average grain size was ~ 315 nm, the size of the Al₂Cu precipitates in the GB was not changed. The sizes and the volume fraction of the Al₃Zr particles were neither changed.

The value of the dislocation density (L_{dis}) in the AG + HPT state was $\sim 2.6 \cdot 10^{13} \text{ m}^{-2}$. After the low-temperature annealing, the dislocation density was dropped to $\sim 1.7 \cdot 10^{13} \text{ m}^{-2}$ due to dislocation annihilation during the annealing. The post-annealing additional deformation led to increase in the dislocation density to $\sim 3 \cdot 10^{13} \text{ m}^{-2}$. The study of the sample microstructure in all the three states carried out by the electron microscopy has not revealed lattice dislocations within the grain interior. It can mean that the dislocation density determined by the XRD analysis is mainly related to the grain boundaries and near GB areas [18]. The value of the lattice parameter a in a state after HPT, after annealing and after subsequent deformation, is still almost unchanged, thereby meaning that the Cu concentration in the solid solution differs insignificantly in all the three states.

Previously, when carrying out the uniaxial tensile tests at the room temperature and the strain rate of $5 \cdot 10^{-4} \text{ s}^{-1}$, we had found the significant increase in the plasticity (the plasticization effect (PE)) in the Al–Cu–Zr UFG-alloy, which was structured by HPT and subjected to special DHT [18]. The Fig. 1 designates this state as AG + HPT + AN + 0.25HPT, in this case the plasticity was $\delta \sim 11\%$ while maintaining high strength values: $\sigma_{0.2} \sim 330$ MPa, $\sigma_{UTS} \sim 465$ MPa. At the same time, after annealing the plasticity sharply reduced to 1–2% (the AG + HPT + AN state in the Fig. 1).

The Fig. 2 shows the stress–strain diagrams for the samples of the Al–Cu–Zr alloy in the AG + HPT and AG + HPT + AN + 0.25HPT states, which were obtained at the different strain rates. Since all the UFG-samples of the Al–Cu–Zr alloy in the AG + HPT + AN state have very low plasticity ($\delta < 2\%$) at all the strain rates under study, the main focus was on the study of the alloy samples after HPT (the AG + HPT state) and after annealing and subsequent additional deformation (the AG + HPT + AN + 0.25HPT state).

The Table 2 shows the values of the main mechanical characteristics, such as the conventional yield stress $\sigma_{0.2}$, the ultimate tensile strength σ_{UTS} , the elongation to failure δ and

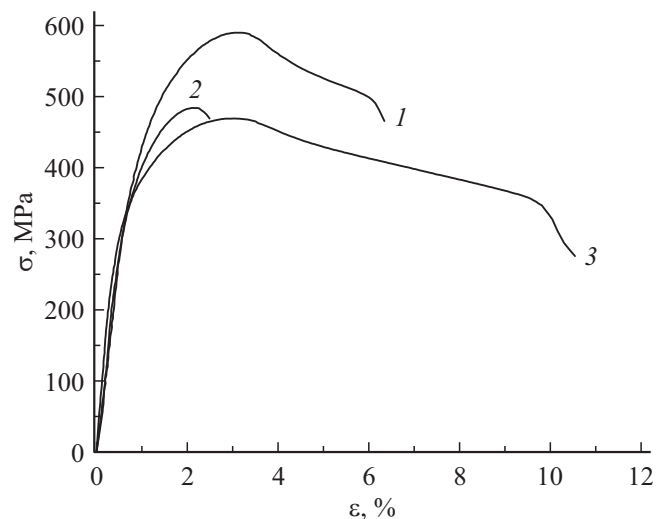


Figure 1. The stress-strain curves obtained at the strain rate of $5 \cdot 10^{-4} \text{ s}^{-1}$ for the Al–1.47Cu–0.34Zr (wt%) alloy in the following states: 1 — AG + HPT; 2 — AG + HPT + AN; 3 — AG + HPT + AN + 0.25HPT.

the uniform elongation δ_1 , determined from the analysis of the strain curves for the corresponding strain rates ε' .

With increase of the strain rate ε' in tension, an increase in the strength characteristics of the UFG alloy is observed in both states AG + HPT and AG + HPT + AN + 0.25HPT (Table 2 and Fig. 2). For the AG + HPT state, the conventional yield stress $\sigma_{0.2}$ increases from 320 to 430 MPa with increase in the strain rate in all the range under study (Fig. 3, a). The ultimate tensile strength σ_{UTS} first increases from 520 to 570 MPa with increase in the strain rate from 10^{-4} to $5 \cdot 10^{-4} \text{ s}^{-1}$; however, further increase in the strain rate to 10^{-2} s^{-1} does not lead to its increase (Fig. 3, b). The trend of change of the strength characteristics of the UFG-alloy in the AG + HPT + AN + 0.25HPT state is similar to that in the AG + HPT state. The magnitudes $\sigma_{0.2}$ and σ_{UTS} of the AG + HPT + AN + 0.25HPT samples are somewhat lower than those of the AG + HPT samples within the whole range of the values ε' under study (Fig. 3), but are still at a fairly high level.

With increase in the strain rate, the plasticity δ of the alloy in the AG + HPT state is steadily decreasing from ~ 6 to $\sim 1\%$ (Fig. 4). At the same time, the uniform elongation δ_1 with increase in the strain rate from 10^{-4} to 10^{-3} s^{-1} is decreasing from ~ 3.2 to $\sim 2.0\%$, while with

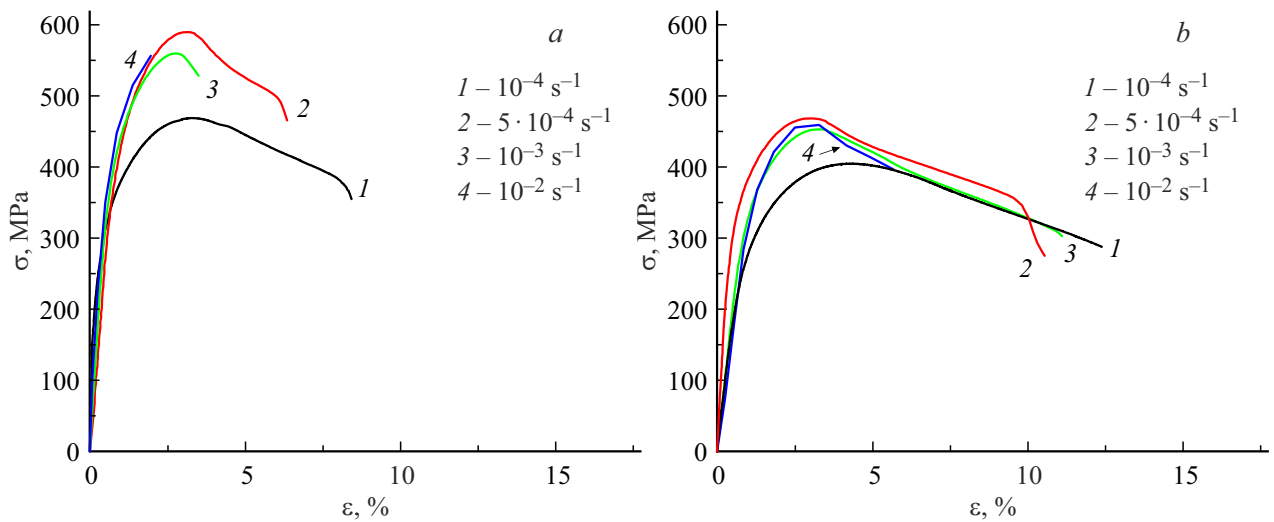


Figure 2. Stress–strain diagrams at the various strain rates ε' for the Al–1.47Cu–0.34Zr (wt%) alloy in the states *a* — AG + HPT and *b* — AG + HPT + AN + 0.25HPT.

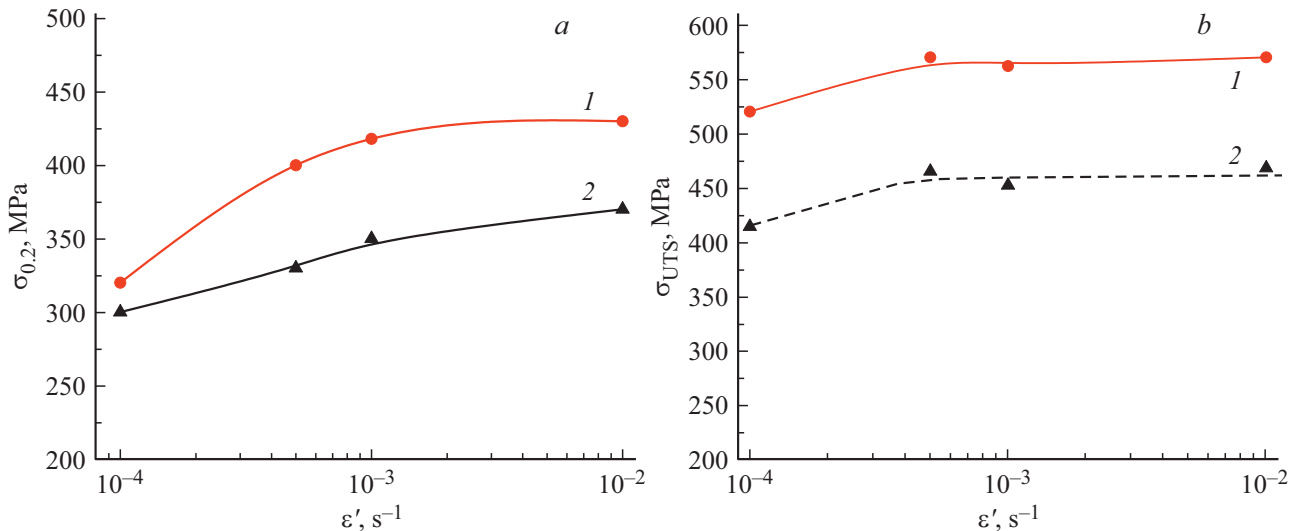


Figure 3. Dependences of the conventional yield stress (*a*) and the ultimate tensile strength (*b*) on the strain rate for the Al–1.47Cu–0.34Zr (wt%) alloy in the AG + HPT (1) and AG + HPT + AN + 0.25HPT states (2).

its further increase to 10^{-2} s^{-1} the samples exhibit almost brittle fracture.

After special DHT (the AG + HPT + AN + 0.25HPT state), the UFG alloy exhibits the high plasticity δ ($> 10\%$) within the wide range of the strain rates 10^{-4} – 10^{-3} s^{-1} . With further increase in the strain rate to 10^{-2} s^{-1} δ decreases to $< 5\%$. However, this plasticity value is significantly higher than the value of δ at the similar strain rate in the AG + HPT state, when the samples exhibit almost brittle fracture. The obtained results mean that the Al–1.47Cu–0.34Zr (wt%) alloy with the UFG-structure after special DHT demonstrates the plasticization effect at all the studied strain rates in comparison with the UFG-state before DHT. It should be noted that DHT application leads

to a small increase of the uniform elongation δ_1 within the strain rate range $5 \cdot 10^{-4}$ – 10^{-2} s^{-1} (Table 2).

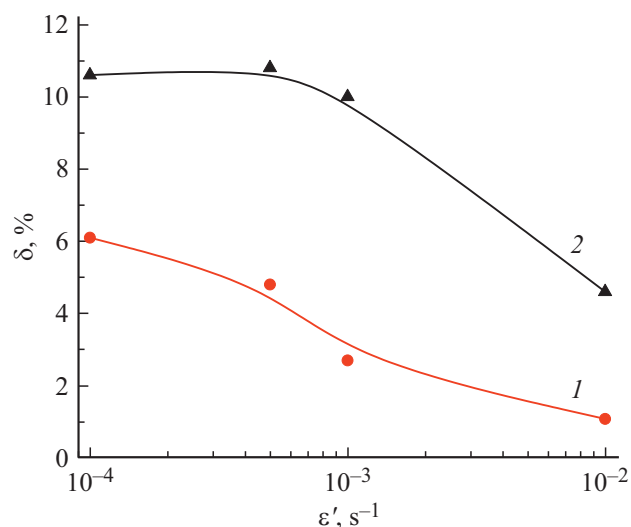
In order to more deeply understand the nature of the increased plasticity effect due to treatment of „annealing and subsequent deformation“, based on the data of Table 2 and using the expression $m = \left(\frac{d \ln \sigma}{d \ln \varepsilon'}\right)_\varepsilon$ [22,26,31], the strain-rate sensitivity coefficient m was determined within the rate range 10^{-4} – 10^{-2} s^{-1} for the AG + HPT and AG + HPT + AN + 0.25HPT states. The results are shown in the Fig. 5, they relate to the deformation of $\varepsilon = 1\%$. As it is shown in the papers [26,32], the dependence of the strain-rate sensitivity coefficient on the deformation in UFG Cu [32], the UFG aluminum alloys [26,33] is very weak. In all the range of the rates under study, the strain-rate sensitivity coefficient for the alloy at the

Table 2. Mechanical properties of the Al–Cu–Zr alloy in the different states as determined at the different strain rates

| Material | State | $\dot{\epsilon}'$, s ⁻¹ | $\sigma_{0.2}$, MPa | σ_{UTS} , MPa | δ , % | δ_1 , % |
|----------|-------------------------|-------------------------------------|----------------------|----------------------|--------------|----------------|
| Al–Cu–Zr | AG + HPT | 10 ⁻⁴ | 320 ± 11 | 520 ± 25 | 6.1 ± 4.9 | 3.2 ± 0.2 |
| | | 5 · 10 ⁻⁴ | 400 ± 16 | 570 ± 6 | 4.8 ± 2.0 | 2.3 ± 0.2 |
| | | 10 ⁻³ | 420 ± 10 | 565 ± 10 | 2.7 ± 0.2 | 2.0 ± 0.1 |
| | | 10 ⁻² | 430 ± 40 | 570 ± 19 | 1.1 ± 0.7 | – |
| | AG + HPT + AN + 0.25HPT | 10 ⁻⁴ | 300 ± 14 | 415 ± 6 | 10.6 ± 1.9 | 3.2 ± 0.3 |
| | | 5 · 10 ⁻⁴ | 330 ± 15 | 465 ± 5 | 10.8 ± 1.4 | 2.5 ± 0.3 |
| | | 10 ⁻³ | 350 ± 5 | 455 ± 6 | 10.0 ± 1.5 | 2.3 ± 0.3 |
| | | 10 ⁻² | 370 ± 18 | 470 ± 8 | 4.6 ± 1.9 | 1.8 ± 0.3 |

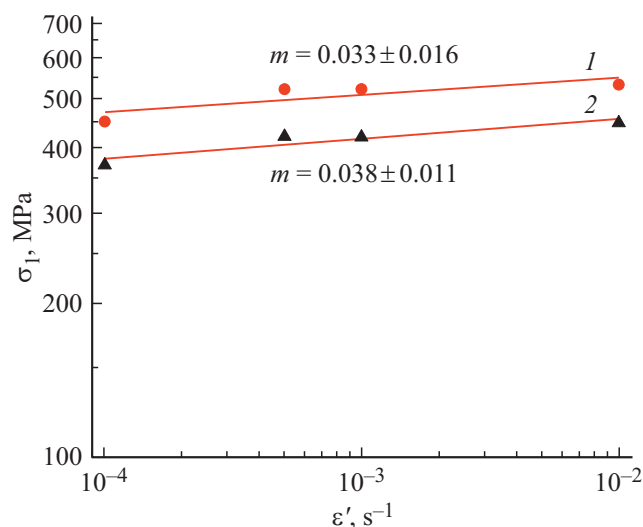
AG + HPT state is equal to $m = 0.033 \pm 0.016$ (Fig. 5). The obtained value well agrees with the literature data [34–36], which show that the value of the strain-rate sensitivity coefficient for the UFG-metals with the FCC lattice is within the range ~ 0.01 – 0.03 . The values of $m \sim 0.03$ and ~ 0.04 were obtained at the room temperature for the high-purity (4N) Al structured by the HPT [19] and for the commercially pure UFG Al (99.5%) structured by the equal channel angular pressing (ECAP), respectively [27]. For the 6082 aluminum alloy in the UFG-state formed by ECAP, the study [26] has obtained the value $m = 0.03$. Such a low value $m = 0.02$ was obtained for the pure Al (99.99%) structured by ECAP within the strain rate range $8.6 \cdot 10^{-4}$ – $3.1 \cdot 10^{-5}$ s⁻¹, while for $\dot{\epsilon}' < 3.1 \cdot 10^{-5}$ s⁻¹, it was an evident increase of m to 0.08, which is correlated to intensification of the grain boundary sliding (GBS) at the low strain rates.

The DHT application has almost not changed the strain-rate sensitivity coefficient: in the AG + HPT + AN + 0.25HPT state the strain-rate sensitivity coefficient is at the same level $m = 0.038 \pm 0.011$ (taking into account

**Figure 4.** Plasticity dependences on the strain rate for the Al–1.47Cu–0.34Zr (wt%) alloy in the different states: 1 — AG + HPT, 2 — AG + HPT + AN + 0.25HPT.

scattering of the experimental data) in all the rate range under study (Fig. 5). According to the studies [1,19,37], the high plasticity or even superplasticity in the Al-based UFG-alloys is manifested significantly due to GBS, which contribution to the total process of the plastic deformation may reach $\sim 60\%$ [1,24]. Usually, intensification of the GBS processes leading to the significantly increased plasticity or even superplasticity in the UFG-alloys is characterized by higher values of the strain-rate sensitivity coefficient $m \sim 0.1$ – 0.3 [22,23,33,37,38]. In both the AG + HPT and AG + HPT + AN + 0.25HPT states, the values of the strain-rate sensitivity coefficient m for the Al–1.47Cu–0.34Zr (wt%) alloy (which are determined in this study) are close and significantly lower. It indicates that the plasticization effect found by us, which is caused by the additional DHT, is not correlated to the intensification of the GBS process.

At the same time, the significantly increased plasticity while maintaining the high level of strength after DHT well agrees with the theoretical model proposed for UFG Al, which describes the PE [12,13]. According to this model,

**Figure 5.** Flow stress dependences at $\epsilon = 1\%$ on the strain rate in the logarithm coordinates for the Al–1.47Cu–0.34Zr (wt%) alloy in the states: 1 — AG + HPT, 2 — AG + HPT + AN + 0.25HPT.

the plastic deformation in UFG Al structured by HPT is implemented by emission of the lattice dislocations from triple junctions. After HPT processing of Al the grain boundaries are in the non-equilibrium state — they contain extrinsic, introduced grain boundary dislocations (GBD), which are pressed by the external shear stress against the GB triple junctions, thereby forming dislocation pile-ups. Such grain boundary dislocation pile-ups (at the triple junctions) lead to the reduced value of the external stress required to emit the dislocations, i.e. it simplifies the process of dislocation emission from the grain boundaries (the triple junctions) and allows emitting a significantly bigger number of dislocations, which slide along the grain and incorporate into the opposite grain boundaries. According to this model, the low plasticity in the state after the short-term low-temperature annealing is attributed to reduced GBD density (relaxation of the non-equilibrium grain boundaries) and therefore, the increased external stress is required to emit the dislocations from the grain boundaries and a reduced number of the lattice dislocations is emitted. The increased plasticity in the state after the annealing and subsequent small deformation is associated with introducing the additional density of the dislocations into the grain boundaries, thereby leading to the increased number of dislocations, which can form pile-ups under the external stress.

The results of the microstructure studies of the Al–Cu–Zr alloy in all the states under study — AG + HPT, AG + HPT + AN and AG + HPT + AN + 0.25HPT (Table 1) — well agree with this model: the annealing leads to reduction of the dislocation density in the grain boundaries and near the GB areas, so does the subsequent HPT deformation by the 0.25 revolution — to the significant increase thereof [18]. Besides the increased dislocation density, the dislocation structure of the grain boundaries in the AG + HPT + AN + 0.25HPT state may differ from that in the AG + HPT state, thereby affecting, in turn, formation of the pile-ups of the grain boundary dislocations at triple junctions under external stress.

The impact of the strain rate on the PE can also be explained within the above-discussed model [12,13] with the assumption of thermally activated sliding of the extrinsic grain boundary dislocations [39]. At the high strain rate, 10^{-2} s^{-1} , the plasticity starts sharply reducing from ~ 11 to $\sim 5\%$. The paper [39] has shown for UFG CP Al structured by HPT that the upper time limit required to form the GB dislocation pile-ups at the room temperature is $\sim 6 \text{ s}$. Taking into account that during the sample mechanical tests in the AG + HPT + AN + 0.25HPT state at the strain rate of 10^{-2} s^{-1} the reaching of the flow stress takes the comparable time of ($\sim 5\text{--}6 \text{ s}$), it can be assumed that within this time the dislocations fail to form fairly strong pile-ups in the grain boundaries, thereby leading to the lower plasticity and possible suppression of the plasticization effect at further increase in the strain rate. Moreover, in contrast to UFG Al, the grain boundaries in the Al–Cu–Zr UFG-alloy contain the nanosized precipitates of the Al_2Cu secondary phase, which can affect the time of formation of the pile-ups

of grain boundary dislocations when the sample is loaded. At the lower strain rates of $10^{-4}\text{--}10^{-3} \text{ s}^{-1}$, there is enough time to form the pile-ups until reaching the yield stress, so the plasticity value δ remains the same within this range of the strain rates.

Conclusion

For the first time the impact of the strain rate on the plasticization effect (PE) of the ultrafine-grained alloy (UFG) Al–1.47Cu–0.34Zr (wt%) structured by the high pressure torsion has been studied. The plasticity in the UFG alloy with $\delta \sim 5\%$ in the state after HPT was increased to the values of $\delta \sim 11\%$ while maintaining the high level of strength ($\sigma_{\text{UTS}} \sim 465 \text{ MPa}$) due to the additional deformation-heat treatment (DHT) consisting of the low-temperature annealing at 125°C and the additional HPT by the 0.25 revolution. It is shown that the plasticity increased due to DHT is maintained within a large range of the strain rates ($10^{-4}\text{--}10^{-3} \text{ s}^{-1}$). With further increase in the strain rate to 10^{-2} s^{-1} , the plasticity significantly decreases.

For the first time, the values of the strain-rate sensitivity coefficient m have been determined for the samples of the Al–1.47Cu–0.34Zr (wt%) alloy in the states before and after DHT. In both the states, the coefficient m has close values of $m = 0.033\text{--}0.038$. Since the value of the coefficient m is still low and almost the same after DHT, it may be concluded that the GBS process is not responsible for the effect of increased plasticity due to the additional deformation. Suppression of the plasticization effect at high strain rates is discussed within the model [12,13] with the assumption of thermally activated sliding of the introduced grain boundary dislocations [39], and forming pile-ups at the triple junctions of the grain boundaries and emitting lattice dislocations in grain interior. We assume that with increase of the strain rate above a certain critical value, there is not enough time to form dislocation pile-ups and their role of emitting dislocations from the grain boundaries decreases and, therefore, the plasticization effect is suppressed. The presence of the (Al_2Cu) secondary phase precipitates in the grain boundaries in the UFG Al–Cu–Zr alloy seem to lead to deceleration of the process of the dislocation pile-ups formation at the grain boundaries, which may affect the character of the $\delta(\epsilon')$ dependence in the alloy in comparison with UFG CP Al, which requires an experimental check and further studies to be carried out.

Conflict of interest

The authors declare that they have no conflict of interest.

References

- [1] K. Edalati, Z. Horita, R.Z. Valiev. *Sci. Rep.* **8**, 1, 1 (2018).
- [2] Y. Huang, T.G. Langdon. *Mater. Today.* **16**, 3, 85 (2013).

- [3] I.A. Ovid'ko, R.Z. Valiev, Y.T. Zhu. *Prog. Mater. Sci.* **94**, 462 (2018).
- [4] I. Sabirov, M.Y. Murashkin, R.Z. Valiev. *Mater. Sci. Eng. A* **560**, 1 (2013).
- [5] B.Q. Han, J.Y. Huang, Y.T. Zhu, E.J. Lavernia. *Acta Mater.* **54**, 11, 3015 (2006).
- [6] Z. Lee, V. Radmilovic, B. Ahn, E.J. Lavernia, S.R. Nutt. *Met. Mater. Trans. A* **41**, 4, 795 (2010).
- [7] Z. Lee, D.B. Witkin, V. Radmilovic, E.J. Lavernia, S.R. Nutt. *Mater. Sci. Eng. A* **410**, 462 (2005).
- [8] V.L. Tellkamp, E.J. Lavernia, A. Melmed. *Metall. Mater. Trans. A* **32**, 9, 2335 (2001).
- [9] Y.H. Zhao, X.Z. Liao, S. Cheng, E. Ma, Y.T. Zhu. *Adv. Mater.* **18**, 17, 2280 (2006).
- [10] S.H. Wu, H. Xue, C. Yang, J. Kuang, P. Zhang, J.Y. Zhang, Y.J. Li, H.J. Roven, G. Liu, J. Sun. *Scripta Mater.* **202**, 113996 (2021).
- [11] A.M. Mavlyutov, T.A. Latynina, M.Yu. Murashkin, R.Z. Valiev, T.S. Orlova. *Physics of the Solid State* **59**, 10, 1949 (2017).
- [12] N.V. Skiba, T.S. Orlova, M.Y. Gutkin. *Phys. Solid State* **62**, 11, 2094 (2020).
- [13] T.S. Orlova, N.V. Skiba, A.M. Mavlyutov, M.Y. Murashkin, R.Z. Valiev, M.Y. Gutkin. *Rev. Adv. Mater. Sci.* **57**, 2, 224 (2018).
- [14] A.M. Mavlyutov, T.S. Orlova, E.Kh. Yapparova. *Pis'ma v ZhTF* **46**, 18, 30 (2020) (in Russian).
- [15] Aluminium and aluminium alloys — Chemical composition and form of wrought products — Part 3: Chemical composition and form of products. German version EN 573-3:2009.
- [16] *Mezhhgosudarstvenny standart. Alyuminiy i splavy alyuminievye deformiruemye. Marki. GOST 4784-2019* (2019) (in Russian).
- [17] *Alloying: understanding the basics.* / Ed. J.R. Davis. ASM International (2001).
- [18] T.S. Orlova, D.I. Sadykov, D.V. Danilov, N.A. Enikeev, M.Yu. Murashkin. *Mater. Lett.* **303**, 130490 (2021).
- [19] N.Q. Chinh, T. Csanádi, T. Györi, R.Z. Valiev, B.B. Straumal, M. Kawasaki, T.G. Langdon. *Mater. Sci. Eng. A* **543**, 117 (2012).
- [20] N.Q. Chinh, P. Szommer, J. Gubicza, M. El-Tahawy, E.V. Bobruk, M.Yu. Murashkin, R.Z. Valiev. *Adv. Eng. Mater.* **22**, 1, 1900672 (2020).
- [21] S.V. Bobylev, N.A. Enikeev, A.G. Sheinerman, R.Z. Valiev. *Int. J. Plast.* **123**, 133 (2019).
- [22] E.V. Bobruk, M.Y. Murashkin, V.U. Kazykhanov, R.Z. Valiev. *Adv. Eng. Mater.* **21**, 1, 1800094 (2019).
- [23] R.Z. Valiev, V.U. Kazykhanov, A.M. Mavlyutov, A. Yudakhina, N.Q. Chinh, M.Yu. Murashkin. *Adv. Eng. Mater.* **22**, 1, 1900555 (2020).
- [24] R.Z. Valiev, M.Yu. Murashkin, A.R. Kilmametov, B. Straumal, N.Q. Chinh, T.G. Langdon. *J. Mater. Sci.* **45**, 17, 4718 (2010).
- [25] E.V. Hart. *Acta Metall. Mater.* **15**, 351 (1967).
- [26] I. Sabirov, Y. Estrin, M.R. Barnett, I. Timokhina, P.D. Hodgson. *Scripta Mater.* **58**, 3, 163 (2008).
- [27] N.V. Isaev, T.V. Grigorova, P.A. Zabrodin. *Physics of the Solid State* **35**, 11, 1151 (2009) (in Russian).
- [28] T.S. Orlova, D.I. Sadykov, M.Yu. Murashkin, V.U. Kazykhanov, N.A. Enikeev. *Physics of the Solid State* **63**, 10, 1572 (2021).
- [29] A.P. Zhilyaev, T.G. Langdon. *Progress. Mater. Sci.* **53**, 6, 893 (2008).
- [30] T.S. Orlova, T.A. Latynina, A.M. Mavlyutov, M.Y. Murashkin, R.Z. Valiev. *J. Alloys Compd.* **784**, 41 (2019).
- [31] M.Y. Alawadhi, Sh. Sabbaghianrad, Y. Huang, T.G. Langdon. *Mater. Sci. Eng.* **802**, 140546 (2021).
- [32] H.S. Kim, Y. Estrin. *Appl. Phys. Lett.* **79**, 25, 4115 (2001).
- [33] K.V. Ivanov, E.V. Naydenkin. *Mater. Sci. Eng. A* **606**, 313 (2014).
- [34] N.Q. Chinh, P. Szommer, T. Csanádi, T.G. Langdon. *Mater. Sci. Eng. A* **434**, 1–2, 326 (2006).
- [35] M.A. Meyer, A. Mishra, D.J. Benson. *JOM* **58**, 4, 41 (2006).
- [36] N.Q. Chinh, G. Vörös, P. Szommer, Z. Horita, T.G. Langdon. *Mater. Sci. Forum* **503**, 1001 (2006).
- [37] P. Kumar, M. Kawasaki, T.G. Langdon. *J. Mater. Sci.* **51**, 1, 7 (2016).
- [38] M. Kawasaki, B. Ahn, P. Kumar, J.I. Jang, T.G. Langdon. *Adv. Eng. Mater.* **19**, 1, 1600578 (2017).
- [39] T.S. Orlova, A.M. Mavlyutov, M.Y. Gutkin. *Mater. Sci. Eng. A* **802**, 140588 (2021).